HHS Public Access

Author manuscript

Behav Neurosci. Author manuscript; available in PMC 2015 December 01.

Published in final edited form as:

Behav Neurosci. 2015 December ; 129(6): 812–821. doi:10.1037/bne0000095.

Neural activation patterns underlying basolateral amygdala influence on intra-accumbens opioid-driven consummatory vs. appetitive high-fat feeding behaviors in the rat

Kyle E. Parker[1,2,3], **Matt P. McCabe**[1,2], **Howard W. Johns**[1,2], **Dane K. Lund**[2,4], **Fiona Odu**[4], **Rishi Sharma**[2,5], **Mahesh M. Thakkar**[5], **DDW Cornelison**[2,4], and **Matthew J. Will**[1,2]

[1]Department of Psychological Sciences, University of Missouri, Columbia, MO

[2]Christopher Bond Life Sciences Center, University of Missouri, Columbia, MO

[3]Interdisciplinary Neuroscience Program, University of Missouri, Columbia, MO

[4]Department of Biological Sciences, University of Missouri, Columbia, MO

[5]Department of Neurology, University of Missouri, Columbia, MO

Abstract

The present study explored the role of the amygdala in mediating a unique pattern of feeding behavior driven by intra-accumbens (Acb) opioid activation in the rat. Temporary inactivation of the basolateral amygdala (BLA), via GABAA agonist muscimol administration prevents increased consumption following intra-Acb opioid administration of the selective μ-opioid agonist D-Ala2, NMe-Phe4, Glyol5-enkephalin (DAMGO), yet leaves food approach behaviors intact, particularly after consumption has ended. One interpretation is that inactivation of the BLA selectively blocks neural activity underlying DAMGO-driven consummatory (consumption), but not appetitive (approach) behaviors. The present experiments take advantage of this temporal dissociation of consumption and approach behaviors to investigate their associated neural activity. Following either intra-Acb saline or DAMGO administration, with or without BLA muscimol administration, rats were given 2hr access to a limited amount of high-fat diet. Immediately following the feeding session, rats were sacrificed and brains assayed for neural activity patterns across critical brain regions known to regulate both appetitive and consummatory feeding behaviors. The results show that intra-Acb DAMGO administration increased c-Fos activation in orexin neurons within the perifornical area of the hypothalamus and that this increase in activation is blocked by BLA muscimol inactivation. Intra-Acb DAMGO administration significantly increased c-Fos activation within dopaminergic neurons of the ventral tegmental area, compared to saline controls, and BLA inactivation had no effect on this increase. Overall, these data provide underlying circuitry that may mediate the selective influence of the BLA on driving consummatory, but not appetitive, feeding behaviors in a model of hedonically-driven feeding behavior.

Corresponding author address: Matthew J. Will, Ph.D., 1201 Rollins St., Department of Psychological Sciences, Christopher Bond Life Sciences Center, University of Missouri, Columbia, Columbia, MO 65211.

The authors declare no conflict of interest.

Keywords

motivated behavior; systems and circuit analysis; laboratory behavior (appetitive/aversive); Animal Model; opioid feeding neural activation pattern

The distributed network contributing to intra-accumbens (Acb) opioid mediated feeding has been extensively examined (Will et al., 2003; Kelley et al., 2005; Zheng et al., 2007; Berridge, 2009), and the contributions of the basolateral amygdala (BLA) have been particularly interesting. Temporary inactivation of the BLA with the $GABA_A$ agonist muscimol prevents the robust increase in high-fat intake following intra-Acb administration of the selective μ-opioid agonist D-Ala2, NMe-Phe4, Glyol5-enkephalin (DAMGO), yet BLA inactivation has no influence on increased feeding driven by acute 24hr food deprivation (Will et al., 2004). This influence of the BLA on specifically mediating a model of hedonic feeding was further characterized to show that BLA inactivation prevented the increased consumption driven by intra-Acb DAMGO, yet left increased food approach behaviors intact, particularly after consumption of the diet had ended. While a more thorough characterization and interpretation of these data has been provided by Will and colleagues (2009), BLA inactivation appears to only interfere with the consumption phase of high-fat feeding behavior, but not the food approach phase driven by opioid activation of the Acb.

Historically, rewarding behaviors have been categorized into an *appetitive* phase, which includes approach behaviors involved in seeking rewarding stimuli such as food, and the *consummatory* phase, which includes behaviors such as the consumption of food (Craig, 1918; Lorenz, 1950). This distinction has been observed for decades and remains popular today as theories of motivation related to food and other rewards evolve (Nicola and Deadwyler, 2000; Berridge, 2004; Kelley et al., 2005; Ball and Balthazart, 2008; Jager & Witkamp, 2014). Attempts at defining the physiology underlying these distinct phases of motivated behavior have included models where treatments have interfered with the expression of one phase without influencing the other (Ikemoto and Panksepp, 1996; Hanlon et al., 2004; Zhang et al., 2003; Jennings et al., 2015). The present study examines the underlying physiology of a unique model of feeding behavior where the consummatory and appetitive phase were dissociated.

The present experiments investigated the neural patterns of activity underlying the appetitive and consummatory feeding behaviors driven by intra-Acb DAMGO. First, the initial finding (Will et al., 2009) was replicated to establish the premise for the second experiment, including the need to determine a proper amount of limited diet to provide in the second study. In the second experiment, following each of four different drug treatment conditions, all subjects were given access to a limited amount of high-fat diet, providing each treatment group except the DAMGO-only treated group, to reach satiety (i.e. amounts observed under ad lib conditions from Experiment 1). Immediately following the 2hr feeding session, rats were sacrificed to capture the neural activity patterns associated with the patterns of behavior displayed. Previous data demonstrated that the entirety of consumption and food hopper approach behavior occurs within the first 30 min of the test session following all

treatments, yet intra-Acb DAMGO, with or without BLA inactivation produce robust levels of food approach behaviors during the final 90 min of the 2hr test session (Will et al., 2009). Therefore, neural activity associated with the motivation to *approach* and *consume* should be represented in rats receiving intra-Acb DAMGO treatment without BLA inactivation. In contrast, neural activity patterns in rats receiving intra-Acb DAMGO treatment with BLA inactivation should reflect equal motivation to *approach*, but reflect reduced motivation to *consume*.

Neural activity was examined in brain regions known to mediate the appetitive and consummatory behaviors of interest, including the ventral tegmental area (VTA), dorsal medial hypothalamus (DMH), perifornical area of the hypothalamus (PeF), and lateral hypothalamus (LH) (Kelley et al., 2005; Zheng et al., 2007; Fields et al., 2007). Intra-Acb DAMGO administration increases c-Fos expression in perifornical hypothalamic neurons and this expression requires orexin signaling within the VTA (Zheng et al., 2007). Collectively, these and other data suggest that this model of palatability-induced feeding through Acb μ-opioid receptor activation may recruit PeF orexin neurons and enhance orexin signaling within the VTA that may in turn modulate DA efflux to the Acb and mPFC, driving feeding behaviors (Fields et al., 2007). The effect of BLA activation being necessary to observe an increase in intra-Acb DAMGO high-fat consumption, but not high-fat approach behaviors, will be explored.

Methods

Rats

Thirty-six adult male Sprague–Dawley rats (Harlan Sprague-Dawley, Inc., Indianapolis, IN) weighing 300–400 g, were housed in pairs in Plexiglas cages in a climate-controlled colony room at a temperature of 22 °C. The rats were maintained on a 12-hr light– dark cycle, and all experiments were conducted during the light phase (0700 –1900) between the hours of 1200 and 1500. Unless otherwise noted, rats had free access to laboratory chow and drinking water before and throughout the experiment. Groups contained 6–8 rats. All experimental procedures were done in accord with protocols approved by the University of Missouri Institutional Animal Care and Use Committee.

Surgery

Rats were anesthetized with a mixture of ketamine and xylazine (90 mg/kg and 9 mg/kg, respectively; Sigma, St. Louis, MO), and 2 sets of guide stainless steel cannulas (23 gauge, 10 mm) were sterotaxically targeted bilaterally above the border of the Acb core and lateral shell and BLA and secured to the skull with stainless steel screws and light curable resin (Dental Supply of New England, Boston). After surgery, wire stylets were placed in the guide cannulas to prevent occlusion. Coordinates for the aimed sites are as follows: Acb: AP, +1.4; ML, ±2.0; DV,-7.8; BLA: AP,-2.8; ML, ±4.7; DV, -8.6 (DV coordinate represents placement of 12.5mm injector needle that extends 2.5mm ventral of the cannula).

Apparatus

Behavioral assessment of feeding took place in a room separate from the colony room in eight Plexiglas (30.5 cm × 24.1 cm × 21.0 cm) feeding chambers (Med Associates, St. Albans, VT). Rats had access to water ad libitum and approximately 35g of palatable diet except where noted. Feeding chambers were equipped with four infrared locomotor activity beams located 6 cm apart across the length of the chamber and 4.3 cm above the floor. An automated weigh scale for the food hopper monitored the consumption of food. An additional infrared beam spanning the entrance of the food hopper determined the number and duration of each head entry into the hopper area. The food hopper and water bottle were located on the same side (opposite corners) of one chamber wall, and a removable waste tray was located beneath the bar floor. The measurements included locomotor activity (number of horizontal beam breaks), duration of hopper entry (average duration of beam break at the entrance of the hopper), hopper entries (number of beam breaks at the entrance to the hopper), and amount consumed (grams of diet consumed). Testing periods consisted of behavioral monitoring in the feeding chambers by a computer running Med-PC software (Med Associates Version IV, St. Albans, VT).

Procedure

Drug Microinjection—D-Ala2, NMe-Phe4, Glyol5-enkephalin (DAMGO; Research Biochemicals, Natick, MA) and muscimol (Sigma, St. Louis, MO) were both dissolved in sterile 0.9% saline. The vehicle control was always sterile 0.9% saline. Infusions were delivered with a microdrive pump (Harvard Apparatus, South Natick, MA), connected by means of polyethylene tubing (PE-10), while rats were gently handheld. Thirty-three-gauge 12.5-mm injectors were used, extending 2.5 mm beyond the end of the guide cannulas. The rate of injection was 0.32 μl/min for the Acb and 0.16 μl/min for the BLA, with the total duration of infusion being 93 s, resulting in 0.5-μl and 0.25-μl volumes, respectively. One additional minute was allowed for diffusion.

Design

Experiment 1: Using a within-subjects design, all groups of rats received each of four drug treatment combinations on four separate treatment days in a counter-balanced order. All behavioral testing for both experiments began 1 week post-surgery in the Med-Associates food intake monitoring chambers. Rats were given access to the diet in these chambers for 2hr daily over 6 consecutive days. On the 5th day, a 10-mm injector was inserted and left in place for 2 min, with no volume injected. On the 6th day, a 12.5-mm injector was inserted, and saline administered for 93 s. On each test day, muscimol (20 ng/0.25 μl/side bilaterally) or saline was infused into the BLA, followed immediately by DAMGO (0.25 mg/0.5 μl/side bilaterally) or saline into the Acb, thus resulting in four possible treatment combinations. The 2hr test session began immediately following the last injection and rats were given ad libitum access to high-fat diet. There was at least 1 day between treatment days.

Experiment 2: Four groups of rats, using a between-subjects design, with each having bilateral cannulas aimed at the Acb and BLA. Rats were given access to the diet in these chambers for 2hr daily over 6 consecutive days and injection procedures were identical to

Experiment 1, however each rat would only be receiving 1 of the 4 possible drug treatments combinations. The consumption of high-fat diet on the 6th day of baseline treatment was used to counter-balance drug treatment assignment to ensure similar baseline control intake patterns. On the 8th day, animals were given 1 of 4 possible drug treatments and access to 8g of palatable diet for 2hr.

Histological Verification of Cannula Placement—Immediately following the 2hr feeding session, animals were removed from the feeding chambers, deeply anesthetized with ketamine and xylazine (90 mg/kg and 9 mg/kg), and transcardially perfused. The brains were removed and immersed in formalin (10%) overnight at 4°C and then cryoprotected by transferring to a sucrose solution (20%) at 4°C. Frozen serial sections (50 μm) were collected through the entire extent of the injection site, mounted on gelatinized slides, and counter-stained with cresyl violet. Cannula placement profiles were then analyzed for accuracy and data from rats with misplaced cannula were not included in the analyses.

Immunohistochemistry—The brains were sliced at 40 μm thickness and stored in 0.1M phosphate buffer solution (PB, pH 7.4) at 4°C. The free floating immunofluorescent staining protocol was as follows: Sections were washed (3 × 10 min) in PBS. Non-specific binding sites were blocked using blocking solution [a mixture 10% normal goat serum (Jackson Immuno Research, West Grove, PA) and 0.3% Triton X-100 (Sigma) in PBS)] for 2 hr. Next, the sections were incubated in a cocktail mixture containing rabbit anti-c-Fos antibody (1: 5000; Calbiochem) and chicken anti-Tyrosine Hydroxylase (VTA) or mouse anti-orexin-A (hypothalamus) overnight. Sections were washed (4 × 30 min) in PBS containing 0.05% Tween-20 (PBST). Next, sections were incubated for 2 hours in a blocking buffer, with a cocktail of secondary antibodies: Alexa Fluor 555 goat Anti-rabbit IgG and Alexa Fluor 488 goat Anti-chicken IgG (Invitrogen). All secondary antibodies were used at the recommended concentration of 1:500. Sections were washed (4 × 30 min) in PBST and PB (2 × 10 min). Sections were mounted on super-frost slides (VWR International, USA) and allowed to dry at room temperature while shielded from light. Using ProLong Anti-fade mounting kit (Invitrogen) the slices were cover slipped and stored at 4°C. All incubations were performed at room temperature except those of the primary antibodies that were incubated at 4°C. To control for variation in the immunohistochemical reaction, tissue from the different treatment groups was reacted together. Additionally, staining was absent in control experiments with omission of the primary antibodies.

Behavioral Statistical Analysis—For experiment 1, all feeding measures for the total 2-hr session and across the various treatment conditions were analyzed with a two-factor within-subject ANOVA (Acb Treatment X Amygdala Treatment), with the levels for each factor being either vehicle or drug. For experiment 2, all feeding measures were analyzed using a two-factor between-subject ANOVA (Acb Treatment X Amygdala Treatment), with the levels for each factor being either vehicle or drug.

Counting procedures, imaging, and statistical analysis—For the quantitative assessment of immunoreactivity expression in the hypothalamus (including the lateral hypothalamus, perifornical area, dorsomedial hypothalamus) and VTA, three anatomically

parallel tissue slices from each hemisphere (6 total per region) were analyzed and averaged. All images were generated through either 4× or 10× objective with a confocal microscope using the imaging software Slidebook 4.3 (Intelligent Imaging Innovations, Denver, CO). Depending on the particular region, fluorescent immunoreactivity within a 40μm slice was imaged for either c-Fos only, c-Fos/TH, or c-Fos/OrexinA labeled channels, separated with an exclusive threshold set. Images were then displayed on a full screen using java-based public domain free software ImageJ (National Institutes of Health, Bethesda, MD, USA), as an image processing and analysis program that allowed tagging each individual neuron and positive staining for each channel was counted in a blind-to-treatment fashion. Neurons were classified as c-Fos only, peptide only, or double-labeled according to the presence of above background antibody reaction product in the cell nucleus.

All areas were designated and mapped using The Rat Brain Atlas (Paxinos & Watson, 1998). Ventral Tegmental Area and Tyrosine Hydroxylase; sections selected were between −5.2 and −5.5mm anterior to bregma. At each level, the region containing tyrosine hydroxylase (TH-IR) cells and c-Fos-IR were counted in both hemispheres. Hypothalamus and Orexin-A; sections selected were between −2.8 and −3.3 mm anterior to bregma. The hypothalamic region (between −2.8 and −3.3 mm) found to contain orexin-A positive cells was divided into three regions from medial to lateral. All cells inside, ventral, and dorsal to the fornix were included the middle region labeled as perifornical (PeF). Orexin-A-labeled cells lateral to this region were included in the lateral hypothalamus (LH), and those medial from the fornix were in the medial group (DMH), which overlapped with the dorsomedial hypothalamus. Neurons were counted in both hemispheres.

Results

All treatment effects are stated in reference to location(s) of drug or vehicle administration (i.e. intra-Acb DAMGO). As all rats were also given access to and consumed a limited amount of high-fat diet, all changes in associated feeding behaviors (Exp. 1 and 2) and neural activation patterns (Exp. 2) are necessarily the combined effect of each respective drug treatment and diet consumed.

Feeding behavior

Experiment 1—Influence of BLA inactivation on high-fat feeding behaviors driven by intra-Acb DAMGO administration.

Consumption: As shown in Fig. 1a, an ANOVA conducted on the food consumption data revealed a significant main effect of Acb treatment ($F(1, 7) = 13.9$, $p < .01$), BLA treatment ($F(1, 7) = 8.6$, $p < .05$), and Acb × BLA treatment interaction ($F(1, 7) = 8.9$, $p < .05$). Post-hoc analysis revealed that intra-Acb DAMGO + intra-BLA saline treatment led to significantly higher consumption levels ($p < .05$) compared to both control treatments (intra-Acb saline + intra-BLA saline; intra-Acb saline + intra-BLA muscimol), and intra-BLA muscimol treatment blocked this increase ($p < .05$).

Food hopper entry duration: As shown in Fig. 1b, an ANOVA conducted on the food hopper entry duration data revealed a significant main effect of Acb treatment ($F(1, 7) =$

36.3, $p < .001$), BLA treatment ($F(1, 7) = 12.1$, $p < .05$), and Acb × BLA treatment interaction ($F(1, 7) = 16.5$, $p < .005$). Post-hoc analysis revealed that intra-Acb DAMGO + intra-BLA muscimol treatment led to significantly higher total food hopper entry duration time compared to all other treatments ($p < .001$), with no other treatment significantly different from each other.

Food hopper entries: As shown in Fig. 1c, an ANOVA conducted on the food hopper entry data revealed a significant main effect of Acb treatment ($F(1, 7) = 10.6$, $p < .05$), while BLA treatment approached significance ($F(1, 7) = 3.89$, $p = .08$), and Acb × BLA treatment interaction ($F(1, 7) = 7.9$, $p < .05$). Post-hoc analysis revealed that intra-Acb DAMGO + intra-BLA muscimol treatment led to significantly more food hopper entries compared to all other treatments ($p < .05$), with no other treatment significantly different from each other.

Locomotor activity: As shown in Fig. 1c, an ANOVA conducted on the food hopper entry data revealed a significant main effect of Acb treatment ($F(1, 7) = 23.5$, $p < .005$), but no main effect of BLA treatment ($F(1, 7) = 1.4$, $p > .05$), and no Acb × BLA treatment interaction ($F(1, 7) = .056$, $p > .05$).

Experiment 2—Influence of BLA inactivation on high-fat feeding behaviors and neural activation patterns driven by intra-Acb DAMGO administration.

Drug treatment assignment was counter-balanced by high-fat intake levels from the 6th day of baseline. These intake levels were as follows: SAL-SAL, 5.1g; SAL-DAM, 4.9g; MUSC-SAL, 4.9g; MUSC-DAM, 4.8g.

Consumption: As shown in Fig. 2a, an ANOVA conducted on the food consumption data revealed a significant main effect of Acb treatment ($F(3, 24)=26.60$, $p < .001$), but no effect of BLA treatment ($F(3, 24)= 0.02$, *ns*) or an Acb × BLA treatment interaction ($F(3, 24)= 0.61$, *ns*).

Food hopper entries: As shown in Fig. 2b, an ANOVA conducted on the total number of hopper entries across the entire feeding session revealed a significant main effect of Acb treatment ($F(3, 24)=8.55$, $p < .01$), but no treatment effect of BLA treatment ($F(3, 24)= 1.68$, *ns*) or an Acb × BLA treatment interaction ($F(3, 24)= 0.39$, *ns*).

Food hopper entry duration: As shown in Fig. 2c, an ANOVA conducted on the total duration of all hopper entries across the entire feeding session revealed a significant main effect of Acb treatment ($F(3, 24)=12.45$, $p = .001$), but no effect of BLA treatment ($F(3, 24)= .62$, *ns*) or an Acb × BLA treatment interaction ($F(3, 24)= 0.07$, *ns*).

Locomotor activity: As shown in Fig. 2d, an ANOVA conducted on the total locomotor activity across the feeding session revealed a significant main effect of Acb treatment ($F(3, 24)=12.93$, $p = .001$), but no effect of BLA treatment ($F(3, 24)= .198$, *ns*) or Acb × BLA treatment interaction ($F(3, 24)= 0.61$, *ns*).

Immunohistochemistry

Ventral Tegmental Area—As shown in Fig. 3a, an ANOVA conducted on c-Fos IR cells in the VTA revealed a significant effect of Acb treatment ($F(3, 24) =,25.67$ $p < .001$), but no effect of BLA treatment ($F(3, 24) =1.13$, ns) or interaction between treatments ($F(3, 24) = 2.80$, ns). An ANOVA conducted on percentage of TH-IR cells that show c-Fos IR revealed an effect of Acb treatment ($F(3, 24) = 6.33$, $p < .05$), but no effect of BLA treatment on the percentage of TH-IR cells that show c-Fos IR ($F(3, 24) = .07$, ns) an no significant interaction between treatments ($F(3, 24) = .63$, ns).

Perifornical hypothalamus—As shown in Fig. 3b, an ANOVA conducted on c-Fos IR in the PeF (region analyzed depicted in Fig. 5b) revealed a significant effect of Acb treatment ($F(3, 24) =30.78$, $p < .001$), BLA treatment ($F(3, 24) = 30.52$, $p < .001$) and an Acb × BLA treatment interaction ($F(3, 24) = 8.75$, $p < .01$). An ANOVA conducted on the percentage of OrxA-IR cells that show c-Fos IR revealed a significant effect of Acb treatment ($F(3, 24) = 55.85$, $p < .001$), BLA treatment ($F(3, 24) = 23.52$, $p < .001$), and an Acb × BLA treatment interaction ($F(3, 24) = 14.32$, $p < .001$). In Figures 5a and 5b, post hoc analyses show that BLA inactivation significantly reduces intra-Acb DAMGO induced c-Fos expression and reduces the number of orexin cells expressing c-Fos ($p < .05$).

Dorsomedial hypothalamus—As shown in Table 1, an ANOVA conducted for the number of c-Fos IR cells in the DMH revealed a significant effect of intra-Acb treatment ($F(3, 24) = 20.19$, $p < .001$), but no effect of intra-BLA treatment ($F(3, 24)= 1.63$, *ns*) or an Acb × BLA treatment interaction ($F(3, 24)= 0.05$, *ns*). An ANOVA conducted on the percentage of OrxA-IR cells that show c-Fos IR revealed a significant effect of Acb treatment ($F(3, 24) = 13.39$, $p < .001$), BLA treatment ($F(3, 24) = 5.85$, $p < .05$), but no Acb × BLA treatment interaction ($F(3, 24) = .89$, $p = .36$).

Lateral hypothalamus—As shown in Table 1, an ANOVA conducted for the number of c-Fos IR cells in the LH revealed no effect of Acb (($F(3,24) = .11$, ns) or BLA treatment (($F(3, 24 = 6.82$, $p < .05$) and no interaction ($F(3,24) = .26$, ns). An ANOVA conducted on the percentage of OrxA-IR cells that show c-Fos IR revealed no significant effect of Acb treatment ($F(3, 24) = .64$, ns), BLA treatment ($F(3, 24) = .08$, ns), or an interaction of treatments ($F(3, 24) = .77$, ns.)

Discussion

Under ad libitum high-fat access conditions, BLA inactivation reduced the increased high-fat intake produced by intra-Acb DAMGO, while leaving exaggerated food hopper approach behaviors intact, confirming the previous report (Will et al., 2009). The second experiment examined these same phenomena, but under limited high-fat diet access conditions, allowing all treatment groups except the intra-Acb DAMGO only treated group, to reach satiety (i.e. consume amounts observed under ad lib conditions in Exp. 1). Intra-Acb saline treated animals, with or without BLA inactivation, consumed similar levels of high-fat diet and displayed similar levels of approach behaviors, as predicted. The two treatment groups of particular interest, those receiving intra-Acb DAMGO with or without BLA inactivation,

consumed nearly all of the high-fat diet available in the first 30 min of the 2hr test session and displayed identical patterns of appetitive behaviors (i.e. number of food hopper entries, food hopper entry duration) over the final 90 min, as predicted. Intra-Acb DAMGO treatment exaggerated both the number and duration of food hopper approach behaviors regardless of BLA inactivation, compared to both intra-Acb saline treated groups as previously reported (Will et al., 2009). Importantly, as observed in experiment 1 and previously (Will et al., 2004, 2009), intra-Acb DAMGO treatment, without BLA inactivation, leads to consumption levels at least double the amount provided under the limited access condition. Therefore, neural activity patterns in rats that received intra-Acb DAMGO treatment without BLA inactivation should reflect both the motivation to *approach* and *consume* additional food beyond what was available. In contrast, neural activity patterns in rats receiving intra-Acb DAMGO treatment, with the BLA inactivated, should reflect an increased motivation to *approach* the food, but a reduced motivation to *consume* additional food, compared to rats treated with intra-Acb DAMGO without BLA inactivation. This is critical to not only the rationale for the design, but the interpretation of the current data. The level of diet available was chosen not only to hold levels of consumption within a limited range across groups, but also to ensure rats in every treatment group, except the DAMGO-only group, reached or neared satiation (as determined by Experiment 1 and previous findings, see Will et al., 2009).

Intra-Acb DAMGO administration significantly increased VTA c-Fos IR in dopaminergic neurons compared to saline control treatment, and intra-BLA muscimol administration had no influence on this increase. Previous research suggests that increases in c-Fos IR in the VTA and in particular, VTA dopamine (DA) neurons, play a central role in reward, motivation, and drug addiction (Park & Carr, 1998; Zhang & Kelley, 2000; Cason et al., 2010). Administration of dopamine antagonists into the Acb blocks appetitive food approach behavior yet has no effect on hunger-induced chow consumption (Baldo et al., 2002) or intra-Acb DAMGO fat consumption (Will et al., 2006). Intra-Acb administration of dopamine agonists increase progressive-ratio responding for a food reinforcer, but have no effect on free feeding (Zhang et al., 2003). These data and others suggest that the exaggerated appetitive food approach behaviors observed in both treatment groups administered intra-Acb DAMGO, with and without BLA inactivation, are mediated by increased activity in VTA dopaminergic neurons.

The pattern of PeF orexin-A neuronal activity matches up with the consumption patterns typically observed following these same treatments effects under ad lib access conditions (Will et al, 2009, 2004), with intra-Acb DAMGO treatment leading to higher consumption than any other treatment. We also found that intra-Acb DAMGO increased DMH c-Fos activity regardless of BLA treatment, but only intra-DAMGO alone increased the proportion of orexin neurons expressing c-Fos compared to controls. Despite its role in DAMGO-induced feeding behavior (Zhang & Kelley, 2000; Will et al., 2003), DAMGO did not significantly increase LH c-Fos activity, although Zhang and Kelley (2000) did not allow animals to reach satiety.

The hypothalamus has long been considered a center for autonomic regulation of energy homeostasis; including feeding regulation, arousal, and reward (Kalra et al., 1999, Harris &

Aston-Jones, 2006). Neurons expressing the orexigenic peptides orexin-A and melanin-concentrating hormone (MCH) are known to densely populate the lateral areas of the hypothalamus (Date et al., 1999), in particular, the perifornical area. The consumption of a high-fat diet observed to be driven by centrally administered orexin-A (Yamanaka et al., 2000) is blocked by prior administration of the opioid antagonist naloxone (Clegg et al., 2002), suggesting an interaction of opioid and orexin peptides in mediating palatable food consumption. Intra-VTA orexin-A administration also excites dopamine neurons (Borgland et al., 2006). Blocking orexin signaling in the VTA reduces DAMGO-induced feeding of a high-fat diet (Zheng et al., 2007), yet to what extent this is through reducing the appetitive behaviors that may contribute to increased consumption is unknown. Therefore, the current finding that the increased VTA dopaminergic activity following intra-Acb DAMGO was unaffected by BLA inactivation, despite reducing PeF orexin activity, raises the importance of behavioral characterization of both the appetitive and consummatory phases of feeding behavior. In addition, these data provide testable hypotheses for examining the influence of PeF orexin and VTA dopaminergic modulation on opioid driven approach and consummatory phases of feeding.

The current study used limited diet access (i.e. grams available) to control for the influence of differential consumption levels following various drug treatments. The study also limited its examination to a single diet; therefore, the possibility remains that opioid-driven feeding of other palatable diets may be regulated similarly. The choice of high fat diet was driven by the past characterizations of the associated network revealed to underlie intra-Acb DAMGO high-fat feeding (Will et al., 2003; Baldo et al., 2013 for review), particularly the role of the BLA (Will et al., 2004, 2009). It is unknown whether the present findings are specific to high-fat diet, or whether they would also be observed using an alternative diet. Interestingly, a recent study found that even among highly palatable diets, there is a marked difference in c-fos activation patterns across key feeding regulatory regions of the mesocorticolimbic circuit (Dela Cruz et al., 2015). Future studies will be required to determine if the present findings are specific to high-fat diets.

In summary, these data provide insight into how the BLA responds to opioid activation of the Acb to specifically drive consumption, but not approach behaviors, associated with a high-fat diet. The data suggest that the consumption behavior driven by intra-Acb DAMGO may be due to increased activity of orexin-A neurons in the PeF, while increased food approach behaviors appear to be associated with increased VTA dopaminergic activity, with BLA activation only required to observe the consumption phase. These data provide a better understanding of two dissociable feeding behaviors within a well-characterized feeding model. This research expands our knowledge of the neural circuitry critical to palatability driven feeding and carry implications for understanding the maladaptive feeding behaviors involved in the development of obesity and food-addiction behaviors.

Acknowledgements

The authors would like to acknowledge the support of grant DA024829 from the National Institute of Drug Abuse to MJW.

References

Badiani A, Leone P, Noel MB, Stewart J. Ventral tegmental area opioid mechanisms and modulation of ingestive behavior. Brain Research. 1995; 670(2):264–276. [PubMed: 7743190]

Baldo BA, Sadeghian K, Basso AM, Kelley AE. Effects of selective dopamine D1 or D2 receptor blockade within nucleus accumbens subregions on ingestive behavior and associated motor activity. Behav Brain Res. 2002 Dec 2; 137(1–2):165–177. [PubMed: 12445722]

Baldo BA, Pratt WE, Will MJ, Hanlon EC, Bakshi VP, Cador M. Principles of motivation revealed by the diverse functions of neuropharmacological and neuroanatomical substrates underlying feeding behavior. Neurosci Biobehav Rev. 2013 Nov; 37(9 Pt A):1985–1998. [PubMed: 23466532]

Ball GF, Balthazart J. How useful is the appetitive and consummatory distinction for our understanding of the neuroendocrine control of sexual behavior? Horm Behav. 2008 Feb; 53(2): 307–311. author reply 315-8. [PubMed: 18045597]

Berridge KC. Motivation concepts in behavioral neuroscience. Physiol Behav. 2004 Apr; 81(2):179–209. Review. [PubMed: 15159167]

Berridge KC. 'Liking' and 'wanting' food rewards: brain substrates and roles in eating disorders. Physiology and Behavior. 2009; 97(5):537–550. [PubMed: 19336238]

Cason AM, Smith RJ, Tahsili-Fahadan P, Moorman DE, Sartor GC, Aston- Jones G. Role of orexin/hypocretin in reward-seeking and addiction: implications for obesity. Physiology and Behavior. 2010; 100(5):419–428. [PubMed: 20338186]

Clegg DJ, Air EL, Woods SC, Seeley RJ. Eating elicited by orexin-A, but not melanin-concentrating hormone, is opioid mediated. Endocrinology. 2002; 143(8):2995–3000. [PubMed: 12130565]

Craig W. Appetites and aversions as constituents of instincts. Biological Bulletin. 1918; 34:91–107.

Date Y, Ueta Y, Yamashita H, Yamaguchi H, Matsukura S, Kangawa K, Sakurai T, Yanagisawa M, Nakazato M. Orexins, orexigenic hypothalamic peptides, interact with autonomic, neuroendocrine and neuroregulatory systems. Proc Natl Acad Sci USA. 1999; 96(2):748–753. [PubMed: 9892705]

Dela Cruz JA, Coke T, Karagiorgis T, Sampson C, Icaza-Cukali D, Kest K, Ranaldi R, Bodnar RJ. c-Fos induction in mesotelencephalic dopamine pathway projection targets and dorsal striatum following oral intake of sugars and fats in rats. Brain Res Bull. 2015 Feb.111:9–19. [PubMed: 25460109]

Fields HL, Hjelmstad GO, Margolis EB, Nicola SM. Ventral tegmental area neurons in learned appetitive behavior and positive reinforcement. Annual Review of Neuroscience. 2007; 30:289–316.

Hanlon EC, Baldo BA, Sadeghian K, Kelley AE. Increases in food intake or food-seeking behavior induced by GABAergic, opioid, or dopaminergic stimulation of the nucleus accumbens: is it hunger? Psychopharmacology (Berl). 2004 Mar; 172(3):241–247. [PubMed: 14598017]

Harris GC, Aston-Jones G. Arousal and reward: a dichotomy in orexin function. Trends in Neuroscience. 2006; 29(10):571–577.

Ikemoto S, Panksepp J. Dissociations between appetitive and consummatory responses by pharmacological manipulations of reward-relevant brain regions. Behav Neurosci. 1996 Apr; 110(2):331–345. [PubMed: 8731060]

Jager G, Witkamp RF. The endocannabinoid system and appetite: relevance for food reward. Nutr Res Rev. 2014 Jun 2; 27(1):172–185. [PubMed: 24933167]

Jennings JH, Ung RL, Resendez SL, Stamatakis AM, Taylor JG, Huang J, Veleta K, Kantak PA, Aita M, Shilling-Scrivo K, Ramakrishnan C, Deisseroth K, Otte S, Stuber GD. Visualizing hypothalamic network dynamics for appetitive and consummatory behaviors. Cell. 2015 Jan 29; 160(3):516–527. [PubMed: 25635459]

Kalra SP, Dube MG, Pu S, Xu B, Horvath TL, Kalra PS. Interacting appetite-regulating pathways in the hypothalamic regulation of body weight. Endocrine Reviews. 1999; 20(1):68–110. [PubMed: 10047974]

Kelley AE, Baldo BA, Pratt WE, Will MJ. Corticostriatal-hypothalamic circuitry and food motivation: integration of energy, action and reward. Physiol Behav. 2005 Dec 15; 86(5):773–795. [PubMed: 16289609]

Lorenz K. The comparative method in studying innate behavior patterns. Symp. Soc. Exp. Biol. 1950; 4:221–268.

Nicola SM, Deadwyler SA. Firing rate of nucleus accumbens neurons is dopamine-dependent and reflects the timing of cocaine-seeking behavior in rats on a progressive ratio schedule of reinforcement. J Neurosci. 2000 Jul 15; 20(14):5526–5537. [PubMed: 10884336]

Park TH, Carr KD. Neuranatomical patterns of Fos-like immunoreactivity induced by a palatable meal and meal-paired environment in saline-and naltrexone treated rats. Brain Research. 1998; 805:169–180. [PubMed: 9733960]

Will MJ, Franzblau EB, Kelley AE. Nucleus accumbens mu-opioids regulate intake of a high-fat diet via activation of a distributed brain network. J Neuroscience. 2003; 23(7):2882–2888. [PubMed: 12684475]

Will MJ, Franzblau EB, Kelley AE. The amygdala is critical for opioid- mediated binge eating of fat. Neuroreport. 2004; 15(12):1857–1860. [PubMed: 15305124]

Will MJ, Pratt WE, Kelley AE. Pharmacological characterization of high-fat feeding induced by opioid stimulation of the ventral striatum. Physiol Behav. 2006 Sep 30; 89(2):226–234. [PubMed: 16854442]

Will MJ, Pritchett CE, Parker KE, Sawani A, Ma H, Lai AY. Behavioral characterization of amygdala involvement in mediating intra-accumbens opioid- driven feeding behavior. Behavioral Neuroscience. 2009; 123(4):781–793. [PubMed: 19634936]

Yamanaka A, Kunii K, Nambu T, Tsujino N, Sakai A, Matsuzaki I, Miwa Y, Goto K, Sakurai T. Orexin-induced food intake involves neuropeptide Y pathway. Brain Research. 2000; 859(2):404–409. [PubMed: 10719096]

Zhang M, Kelley AE. Enhanced intake of high-fat food following striatal mu-opioid stimulation: microinjection mapping and fos expression. Neuroscience. 2000; 99(2):267–277. [PubMed: 10938432]

Zhang M, Kelley AE. Intake of saccharin, salt, and ethanol solutions is increased by infusion of a mu opioid agonist into the nucleus accumbens. Psychopharmacology (Berl). 2002; 159(4):415–423. [PubMed: 11823894]

Zhang M, Balmadrid C, Kelley AE. Nucleus accumbens opioid, GABaergic, and dopaminergic modulation of palatable food motivation: contrasting effects revealed by a progressive ratio study in the rat. Behav Neurosci. 2003 Apr; 117(2):202–211. [PubMed: 12708516]

Zheng H, Patterson LM, Berthoud HR. Orexin signaling in the ventral tegmental area is required for high-fat appetite induced by opioid stimulation of the nucleus accumbens. J of Neuroscience. 2007; 27(41):11075–11108. [PubMed: 17928449]

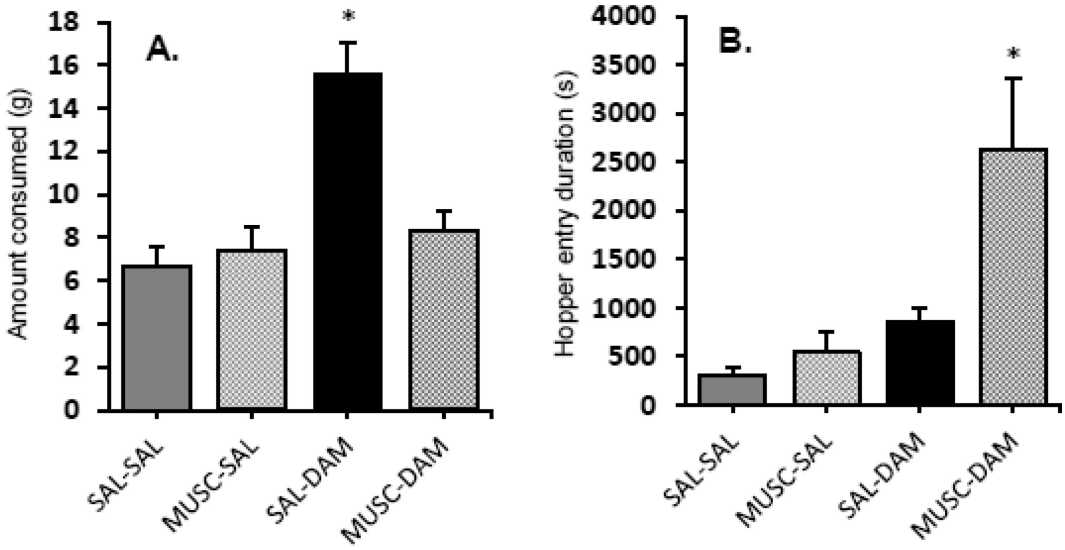

C.

Treatment	Hopper entries	Locomotor
SAL-SAL	133±38	876±134
MUSC-SAL	146±37	601±126
SAL-DAMGO	204±54	1704±243
MUSC-DAMGO	388±70 *	1529±251

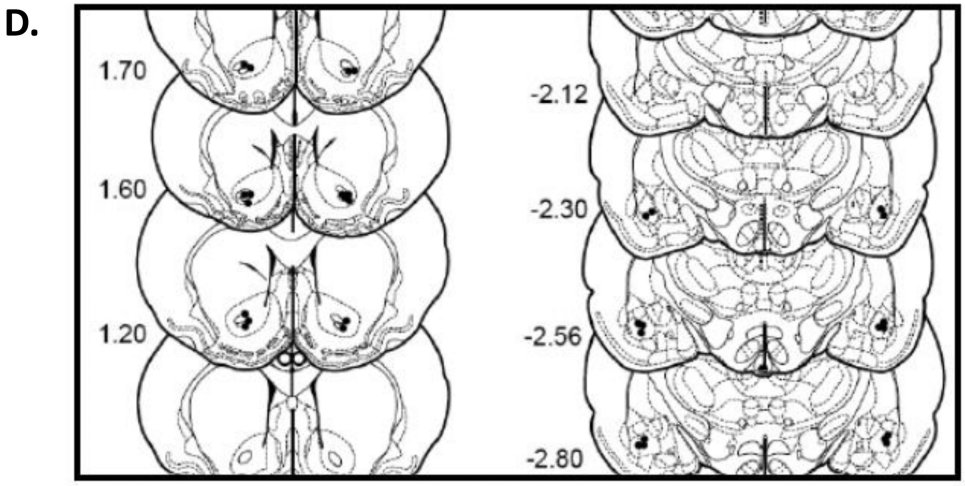

Figure 1.

Behavioral examination: **A)** Amount of high-fat diet consumed (ad libitum access), **B)** total food hopper entry duration, **C)** total number of food hopper entries, and locomotor activity counts (i.e. horizontal beam break). 4 treatments were administered in counter-balanced order, including intra-Acb DAMGO or saline (SAL) immediately after intra-BLA muscimol (MUSC) or SAL. The x-axis labels refer to treatment of the two regions (i.e. BLA treatment - Acb treatment). The y-axis values (**A, B**) represent group means (plus or minus standard error of the mean). Values noted in C represent group means (plus or minus standard error of

the mean). Asterisk (*) represents a significant difference ($p < .05$) between that treatment, compared to all other treatments. **(D)** Placement for Acb and BLA injections are indicated with black circles. Histological figures adapted from The Rat Brain in Stereotaxic Coordinates (4th Ed.), G. Paxinos and C. Watson, 1998.

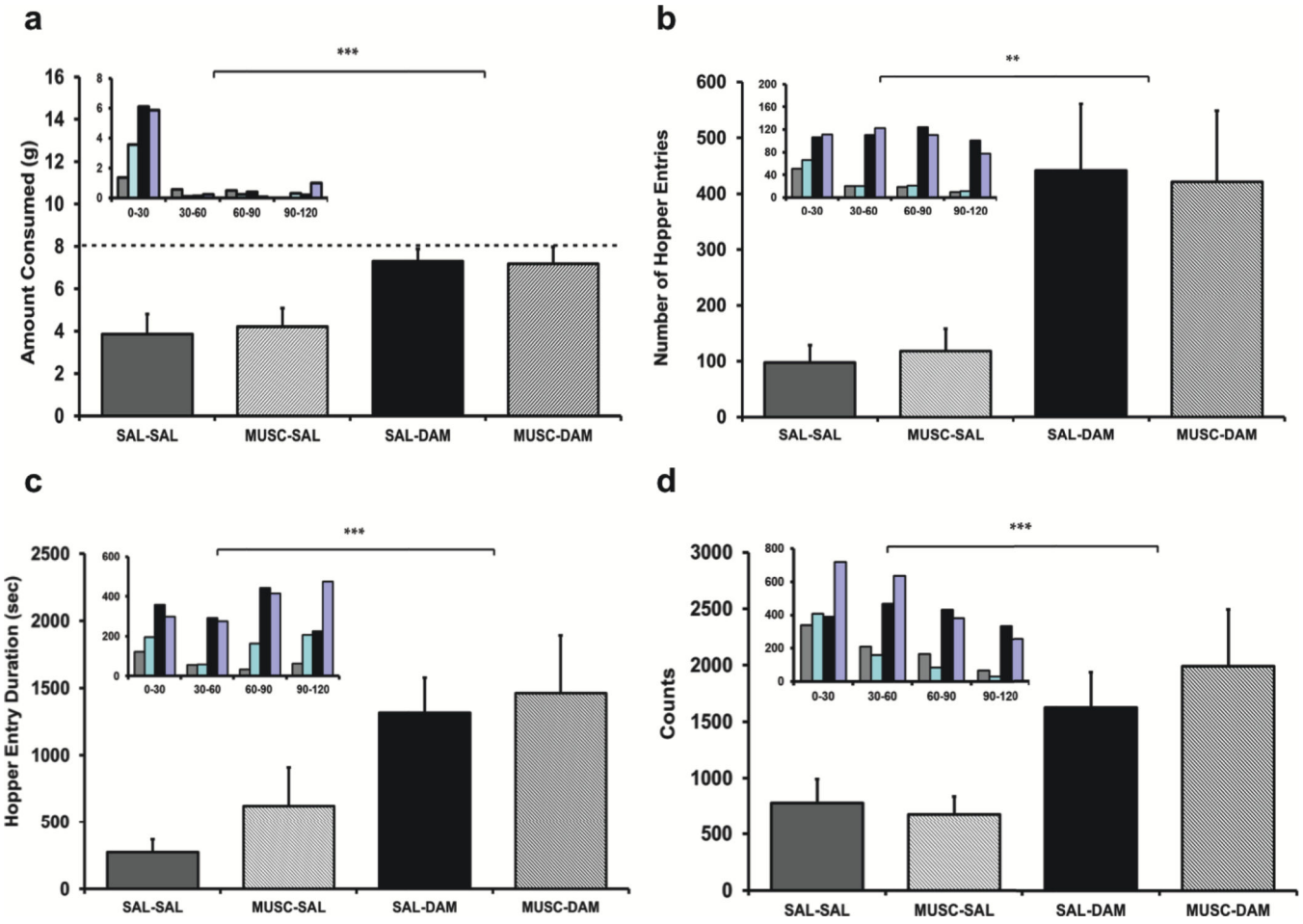

Figure 2.

Behavioral examination: **a)** Amount of high-fat diet consumed (dashed line reflects limited access of 8g); **b)** number of food hopper entries, **c)** total food hopper entry duration, and **d)** locomotor activity counts (i.e. horizontal beam breaks). 4 treatments were administered, including intra-Acb DAMGO or saline (SAL) immediately after intra-BLA muscimol (MUSC) or SAL. The x-axis labels refer to treatment of the two regions (i.e. BLA treatment - Acb treatment). The y-axis values represent group means (plus or minus standard error of the mean). Asterisk represents a significant difference between the intra-Acb DAMGO versus saline administration treatment groups, collapsed across intra-BLA treatment; Level of significance indicated by number of symbols (i.e. ** $p < .01$, and *** $p < .001$).

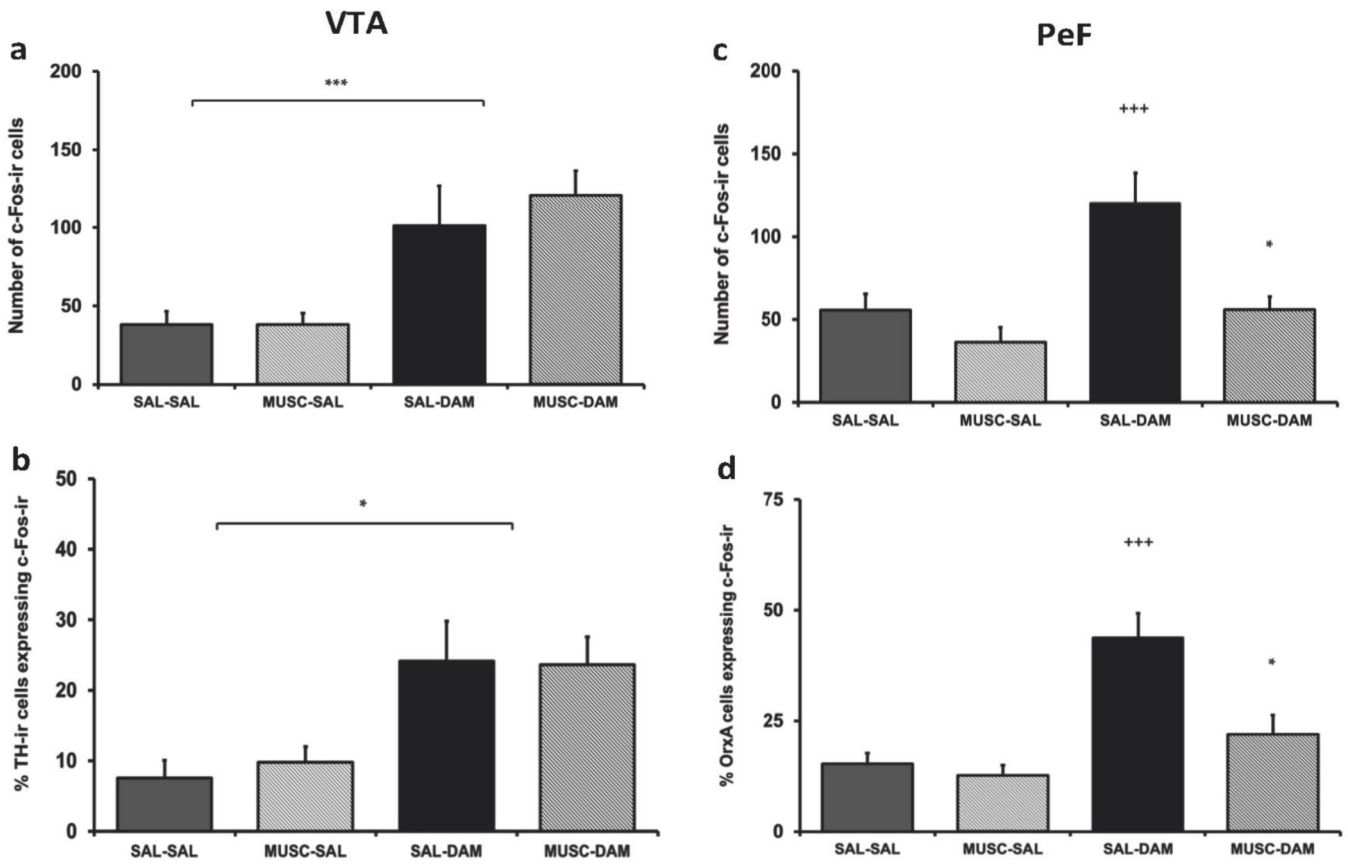

Figure 3.

a) Number of VTA cells expressing c-Fos IR; **b)** Percentage of VTA TH-IR cells expressing c-Fos IR. **c)** Number of cells expressing c-Fos-IR in the perifornical area of the hypothalamus (PeF) **d)** Percentage of PeF Orexin-A IR cells expressing c-Fos-IR. 4 treatments were administered, including intra-Acb DAMGO or saline (SAL) immediately after intra-BLA muscimol (MUSC) or SAL. The x-axis labels refer treatment for the two regions (i.e. Acb treatment-BLA treatment). Values represent group means (plus or minus standard error of the mean). Plus sign represents SAL-DAM versus SAL-SAL; asterisk represents MUSC-DAM versus SAL-DAM. Level of significance indicated by number of symbols (i.e.,* $p < .05$, ** $p < .01$, and *** $p < .001$).

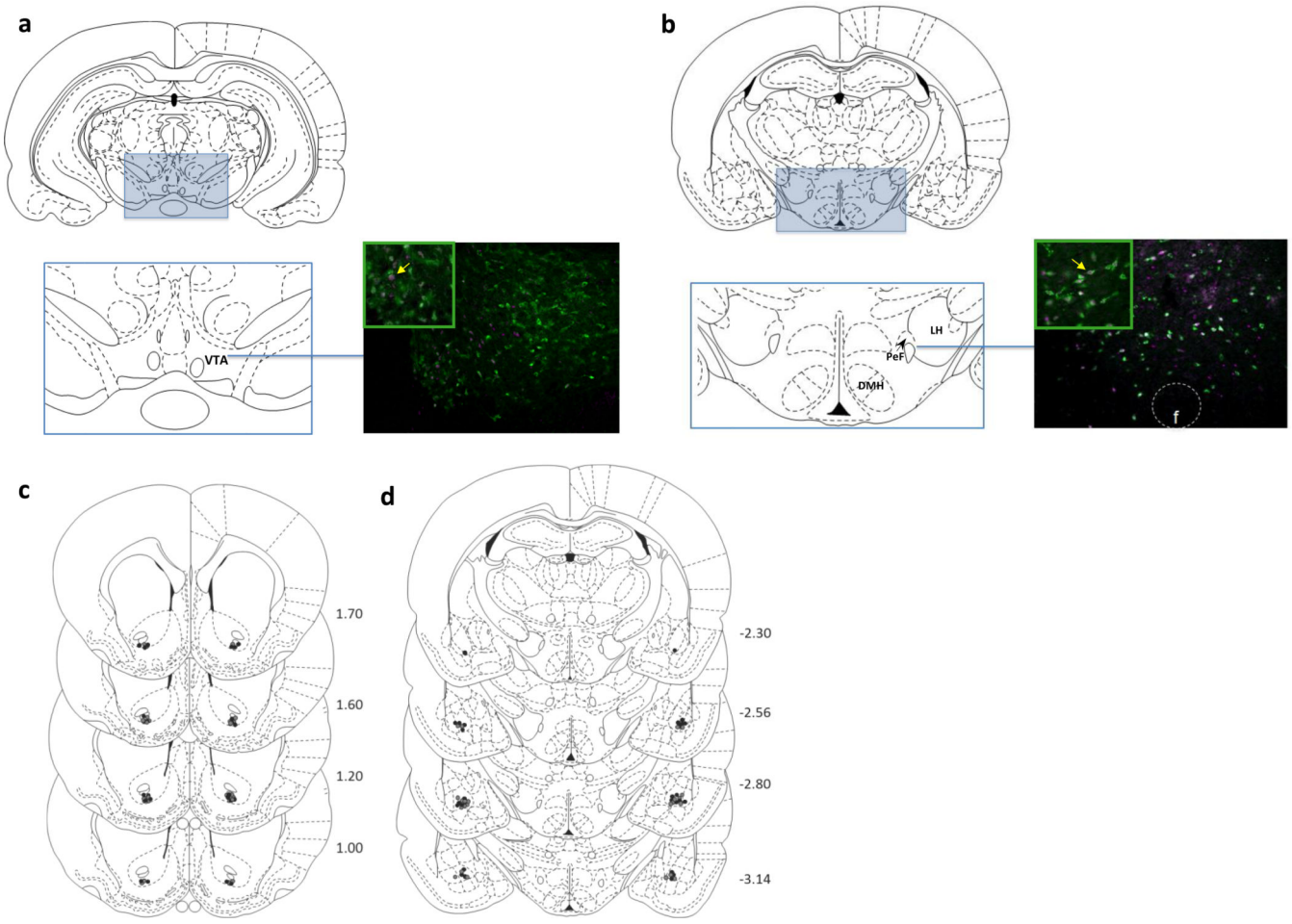

Figure 4.

Schematic line drawings, adapted from Paxinos & Watson (1998) atlas, depicting coronal sections containing analyzed brain regions outlined in blue area (grey area) and enlarged directly below. Regions: **(a)** ventral tegmental area, VTA; **(b)** dorsomedial hypothalamus, DMH; lateral hypothalamus, LH; perifornical hypothalamus, PeF. The immunofluorescence image (10×) of the VTA (panel a) displays an example of distinct TH-immunoreactive cells, falsely colored in green (light grey) c-Fos-IR cells in magenta (dark grey). The yellow arrow in figure **(a)** inset indicates a TH-IR positive cell. The immunofluorescence image of the PeF (4×) region (panel b) displays an example of distinct orexin-immunoreactive cells, falsely colored in green (light grey) and c-Fos-IR cells in magenta (dark grey) (fornix, f). The yellow arrow in figure **(b)** inset indicates Orexin-A IR positive cell. Placement for **(c)** nucleus accumbens (Acb) injections (gray: saline, black: DAMGO) and **(d)** basolateral amygdala (BLA) injections (gray: saline, black: muscimol). Histological figures adapted from The Rat Brain in Stereotaxic Coordinates (4th Ed.), Figures 11, 12, 13, 14, 28, 29, 30, 31, 32 by G. Paxinos and C. Watson, 1998.

Table 1

Number of cells expressing c-Fos-IR (total) in the lateral hypothalamus and dorsomedial hypothalamus and percentage of PeF Orexin-A IR cells expressing c-Fos-IR (% orexin-A). 4 treatments were administered, including intra-Acb DAMGO or saline (SAL) immediately after intra-BLA muscimol (MUSC) or SAL.

Lateral Hypothalamus				
Treatment	Mean (total c-Fos)	SEM (total)	Mean (% orexin-A)	SEM (%)
SAL-SAL	17.71	2.55	16.2	4.5
SAL-MUSC	12.33	2.75	17.4	8.1
DAMGO-SAL	19.85	2.55	19.6	4.7
DAMGO-MUSC	11.87	2.38	17.2	3.8
Dorsomedial Hypothalamus				
Treatment	Mean (total c-Fos)	SEM (total)	Mean (% orexin-A)	SEM (%)
SAL-SAL	38.14	5.09	33.8	14.9
SAL-MUSC	34.50	5.50	34.1^{b}	13.4
DAMGO-SAL	62.14^{a}	5.09	54.6a	6.6
DAMGO-MUSC	56.50^{a}	4.76	39.4a.^{b}	14.2

Values represent group means and standard error of the mean. There were no LH treatment effects. For the DMH results, main treatment effects of Acb treatment (^{b}) and BLA treatments (^{a}) were observed.